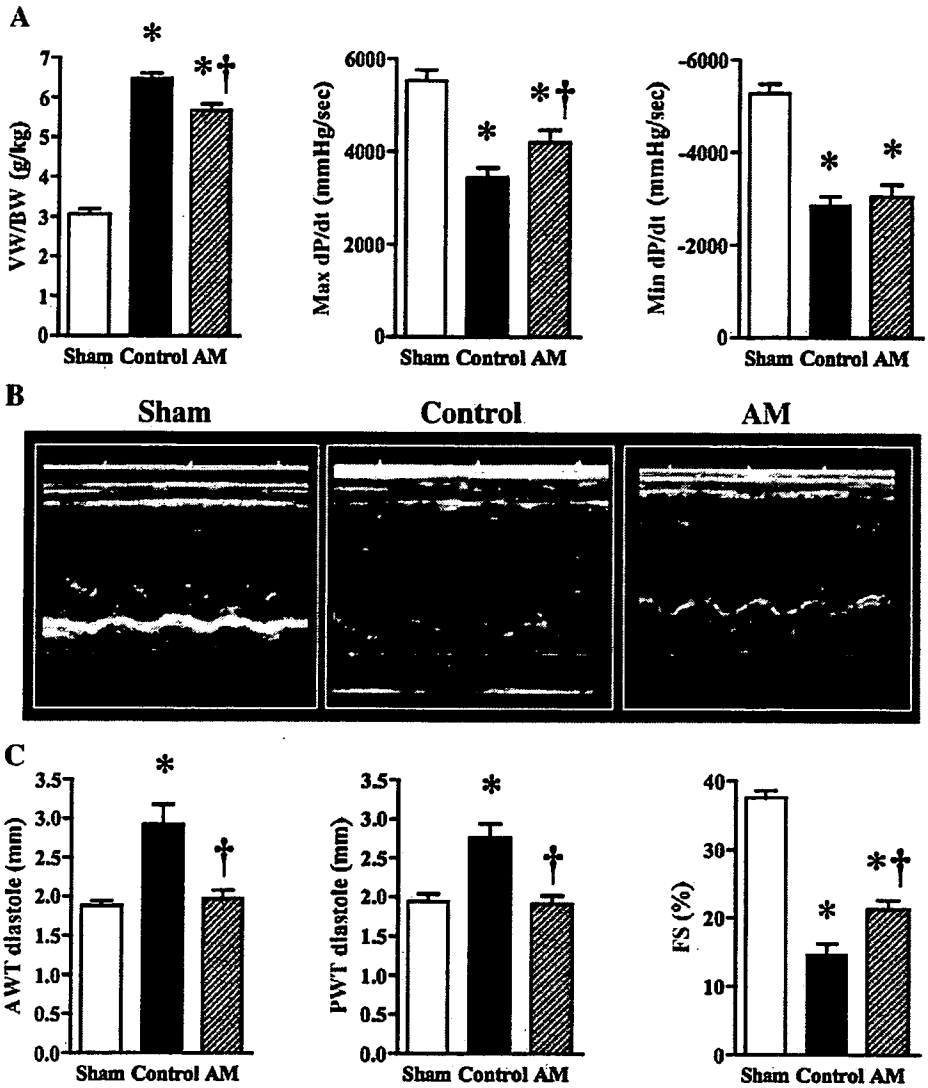

Fig. 6. Effects of AM infusion on physiologic properties and hemodynamic parameters. A: Effects of AM infusion on physiologic properties ($n=7$ in each group). B: Representative echocardiographic images show wall thickening and poor movement in myocarditis and improvement with AM treatment. C: Effects of AM infusion on echocardiographic findings ($n=10$ in each group). VW/BW, ventricular weight/body weight ratio; Max dP/dt, maximum dP/dt; Min dP/dt, minimum dP/dt; AWT, anterior wall thickness; PWT, posterior wall thickness; %FS, %fractional shortening. Data are mean±S.E. *, $P<0.05$ *vs.* sham; †, $P<0.05$ *vs.* control.

ANOVA, followed by Newman–Keuls' test. Comparisons of parameters between two groups were made by Student's *t*-test. A value of $P<0.05$ was considered statistically significant.

3. Results

3.1. Histopathological improvement after AM infusion

Sections of left ventricular tissue demonstrated substantial myocardial necrosis, infiltration of inflammatory cells and edema in the control group, which was significantly limited primarily to areas directly adjacent to arterial vessels with AM treatment (Fig. 1, panel A). Blinded histological grading confirmed decreased myocyte necrosis, granulation, inflammation and tissue edema in the AM group as compared in the control group (Fig. 1, panel B). Picrosirius red staining revealed increased collagen deposition in the control group (Fig. 1, panel C). However, AM infusion attenuated collagen deposition in the myocardium (Fig. 1, panel D).

Table 2
Echocardiographic findings

	Sham	Control	AM
LVDd, mm	4.9±0.1	6.5±0.2*	7.3±0.3*
LVDs, mm	3.1±0.1	5.7±0.2*	5.7±0.3*
EF, %	75±1	35±3*	52±2*†

Sham, sham rats given vehicle; Control, myosin-treated rats given vehicle; AM, myosin-treated rats given AM; LVDd, left ventricular diastolic dimension; LVDs, left ventricular systolic dimension; EF, ejection fraction. Data are mean± S.E. *$P<0.05$ *vs.* sham; †$P<0.05$ *vs.* control. $n=10$ in each group.

3.2. Infiltration of CD68-positive cells in myocardium

A significant decrease in infiltration of CD68-positive inflammatory cells was observed in the AM group as compared to the control group (790±80 *vs.* 1468±109 cells/mm^2; Fig. 2, panel A and B). Sham tissues showed little or no myocardial CD68 positivity (data not shown).

3.3. Expression of MCP-1 after AM infusion

The expression of MCP-1 was increased in myocarditis; it was localized to the vascular endothelium and also in myocytes surrounding and adjacent to the areas of inflammation (Fig. 3, panel A). Heart sections in the AM group showed a partial decrease in MCP-1 expression. Serum MCP-1 level was greatly increased in the control group, whereas a significant decrease was observed in the AM group (Fig. 3, panel B).

3.4. Effects of AM infusion on MMPs and TGF-β expression

Western blotting analysis revealed that myocardial levels of MMP-2 and -9 were significantly increased in the control group. MMP-2 expression was markedly decreased by AM infusion, and MMP-9 expression tended to be decreased after AM infusion (Fig. 4, panel A). Quantitative real-time RT-PCR analysis demonstrated increased expression of TGF-β in the heart of the control group which was significantly attenuated by AM treatment (Fig. 4, panel B). AM infusion did not significantly influence cardiac expression of IL-1β and TNF-α (data not shown).

3.5. Angiogenesis induced by AM infusion

To determine the effect of AM treatment on angiogenesis, vWF-stained heart sections were subjected to capillary density counting. Capillary density was increased in the control group, particularly in areas directly adjacent to tissue necrosis (1146± 57 *vs.* 782±21 cells/mm^2, Fig. 5, panel A and B). However, in AM-treated tissues, capillary density was further significantly increased not only in the peri-necrotic areas but also in apparently healthy myocardium (1347±82 *vs.* 1146±57cells/mm^2), suggesting that stimulation of angiogenesis was further augmented by AM treatment.

3.6. Heart weight and hemodynamics after AM infusion

The physiological and catheter-derived functional properties on day 21 post-myosin injection are summarized in Table 1 and Fig. 6, panel A. Myocarditic hearts showed significantly increased heart weight to body weight ratio, which was decreased by AM treatment. AM treatment also significantly improved maximum dP/dt. For both minimum dP/dt and LVEDP, we did not find significant differences. On echocardiography, AM administration significantly attenuated increased wall thickness after acute myocarditis. AM significantly improved LV fractional shortening and ejection fraction, although LVDd did not significantly differ between control and AM groups (Table 2 and Fig. 6, panel B and C).

4. Discussion

In the present study, AM treatment showed the following effects in acute myocarditis: 1) reduced necrosis, inflammation and edema in the myocardium; 2) attenuated expression of MCP-1, MMP-2 and TGF-β; 3) increased capillary density suggestive of angiogenesis; and 4) improved cardiac function.

This experimental autoimmune myocarditis model is triphasic, consisting of an antigen priming phase from days 0 to 14, an autoimmune response phase from days 14 to 21, and a reparative phase thereafter, associated chronically with a dilated cardiomyopathy phenotype [20]. MCP-1 expression is increased in the heart from days 15 to 27 post-myosin injection, and serum MCP-1 level is elevated from days 15 to 24 [21]. We treated rats with AM at 1 week after myosin injection, corresponding to an early time point in the disease process. Pathological examination demonstrated that infusion of AM attenuated myocyte necrosis and inflammation in acute myocarditis. This observation was supported by a decrease in infiltration of CD68-positive inflammatory cells in the myocardium. Interestingly, both MCP-1 expressions in the myocardium and serum MCP-1 level were decreased after AM infusion. MCP-1 is a member of the C–C subfamily of chemokines with chemoattractant activity for major inflammatory cells such as monocytes and T lymphocytes [22], and this model of acute myocarditis has previously been shown to be associated with MCP-1 [21]. Thus, the decrease in CD68-positive cell infiltration in the myocardium following this treatment may be attributable to inhibition of MCP-1 production by AM. The inhibitory effect of AM on MCP-1 expression is consistent with a previous *in vitro* study showing that AM inhibited pressure-induced MCP-1 expression in mesangial cells [23]. Recently, it has been demonstrated that AM has anti-inflammatory effects through modulation of macrophage migration inhibitory factor secretion [24]. Importantly, overexpression of MCP-1 induces myocarditis and subsequent development of heart failure [25]. These findings suggest that the inhibitory effect on MCP-1 expression and subsequent anti-inflammatory effect of AM are possible mechanisms of the improvement in acute myocarditis.

We found a significant increase in heart weight to body weight ratio and wall thickness 3 weeks after myosin injection. These results indicate exaggerated edematous changes in myocarditic hearts. Infusion of AM reduced overall heart weight to body weight ratio and wall thickness in myocarditic hearts and attenuated histological edematous changes. Earlier studies have demonstrated that AM decreases vascular congestion and endothelial hyperpermeability in the heart [11], reduces hyperpermeability of cultured endothelial cells and inhibits pulmonary edema [26]. Thus, it is interesting to speculate that the attenuation of edematous changes in the

heart may be attributable to reduction of endothelial hyperpermeability by AM.

In the present study, AM infusion significantly increased the capillary density in myocarditic hearts. In fact, earlier studies have demonstrated angiogenic properties of AM *in vitro* and *in vivo* [27–29]. Importantly, improvement in myocardial vascular supply has been shown to decrease necrosis and inflammation in viral myocarditis [30,31]. These results suggest that AM-induced angiogenesis in the myocardium may be responsible for the improvement in acute myocarditis, which was indicated by reduced necrosis and inflammation in myocarditic hearts.

As previously mentioned, experimental autoimmune myocarditis chronically develops into a dilated cardiomyopathy phenotype [20]. MMPs have been associated with left ventricular remodeling [32] and here we showed increased expression of MMP-2 and -9 as well as increased collagen deposition in myocarditic hearts. In the present study, AM treatment significantly reduced both MMP-2 expression and collagen deposition. In addition, our observation demonstrated that the expression of TGF-β, a profibrogenic factor, was also attenuated by AM treatment. It has been demonstrated that AM decreases the expression of TGF-β in experimental mesangioproliferative glomerulonephritis [33]. These results suggest that AM may have beneficial effects on myocardium, possibly through regulation of factors involved in LV remodeling. In the present study, LVDd did not significantly differ between the control and AM groups. However, it should be noted that AM significantly reduced wall thickness possibly due to reduction of myocardial edema, leading to a slight increase in the inner diameter of the LV and a significant increase in ejection fraction. The major effect of AM was to reduce myocardial edema but not remodeling, despite reducing biochemical markers of remodeling.

Earlier studies have shown that short-term infusion of AM decreases arterial pressure and increases cardiac output in patients with acute heart failure [5]. These findings suggest that the improvement in cardiac function after acute myocarditis may be mediated partly by the hemodynamic effects of AM. However, despite the well-characterized vasorelaxant properties of AM [4], there was a significant increase in mean arterial pressure after AM treatment in our model. These findings suggest that AM induced limited direct hemodynamic action. Taking these findings together, the improvement of cardiac function after AM treatment may have been mediated by the improvement of pathological findings including necrosis, inflammation and edema in the myocardium rather than by AM-induced hemodynamic effects.

In conclusion, infusion of AM improved cardiac function and pathological findings including inflammatory infiltration and edema in a rat model of acute myocarditis. The beneficial effects of AM may occur at least in part by inhibitory effects on MCP-1, MMP-2 and TGF-β, and by enhancement of angiogenesis after acute myocarditis. Thus, infusion of AM may be a potent therapeutic strategy for acute myocarditis.

Acknowledgements

This work was supported by research grants for Cardiovascular Disease (16C-6 and 17A-1) and Comprehensive Research on Aging and Health from the Ministry of Health, Labour and Welfare, the Program for Promotion of Fundamental Studies in Health Sciences of the National Institute of Biomedical Innovation (NIBIO); and Health and Labor Sciences Research Grants (Human Genome Tissue Engineering 009).

References

[1] Levi D, Alejos J. Diagnosis and treatment of pediatric viral myocarditis. Curr Opin Cardiol 2001;16:77–83.
[2] Liu Z, Yuan J, Yanagawa B, Qiu D, McManus BM, Yang D. Coxsackievirus-induced myocarditis: new trends in treatment. Expert Rev Anti Infect Ther 2005;3:641–50.
[3] Feldman AM, McNamara D. Myocarditis. N Engl J Med 2000;343: 1388–98.
[4] Kitamura K, Kangawa K, Kawamoto M, Ichiki Y, Nakamura S, Matsuo H, et al. Adrenomedullin: a novel hypotensive peptide isolated from human pheochromocytoma. Biochem Biophys Res Commun 1993;192:553–60.
[5] Nagaya N, Satoh T, Nishikimi T, Uematsu M, Furuichi S, Sakamaki F, et al. Hemodynamic renal and hormonal effects of adrenomedullin infusion in patients with congestive heart failure. Circulation 2000;101:498–503.
[6] Oya H, Nagaya N, Furuichi S, Nishikimi T, Ueno K, Nakanishi N, et al. Comparison of intravenous adrenomedullin with atrial natriuretic peptide in patients with congestive heart failure. Am J Cardiol 2000;86:94–8.
[7] Clementi G, Caruso A, Cutuli VM, Prato A, Mangano NG, Amico-Roxas M. Antiinflammatory activity of adrenomedullin in the acetic acid peritonitis in rats. Life Sci 1999;65:PL203–8.
[8] Okumura H, Nagaya N, Itoh T, Okano I, Hino J, Mori K, et al. Adrenomedullin infusion attenuates myocardial ischemia/reperfusion injury through the phosphatidylinositol 3-kinase/Akt-dependent pathway. Circulation 2004;109:242–8.
[9] Iwase T, Nagaya N, Fujii T, Itoh T, Ishibashi-Ueda H, Yamagishi M, et al. Adrenomedullin enhances angiogenic potency of bone marrow transplantation in a rat model of hindlimb ischemia. Circulation 2005;111: 356–62.
[10] Tsuruda T, Kato J, Kitamura K, Kuwasako K, Imamura T, Koiwaya Y, et al. Adrenomedullin: a possible autocrine or paracrine inhibitor of hypertrophy of cardiomyocytes. Hypertension 1998;31:505–10.
[11] Chu DQ, Smith DM, Brain SD. Studies of the microvascular effects of adrenomedullin and related peptides. Peptides 2001;22:1881–6.
[12] Kodama M, Matsumoto Y, Fujiwara M, Zhang SS, Hanawa H, Itoh E, et al. Characteristics of giant cells and factors related to the formation of giant cells in myocarditis. Circ Res 1991;69:1042–50.
[13] Kodama M, Matsumoto Y, Fujiwara M, Masani F, Izumi T, Shibata A. A novel experimental model of giant cell myocarditis induced in rats by immunization with cardiac myosin fraction. Clin Immunol Immunopathol 1990;57:250–62.
[14] Fairweather D, Kaya Z, Shellam GR, Lawson CM, Rose NR. From infection to autoimmunity. J Autoimmun 2001;16:175–86.
[15] Cunningham MW. T cell mimicry in inflammatory heart disease. Mol Immunol 2004;40:1121–7.
[16] O'Connell JBRD. Myocarditis and specific myocardial diseases. New York: McGraw-Hill; 1994. Pages.
[17] Yanagawa B, Spiller OB, Choy J, Luo H, Cheung P, Zhang HM, et al. Coxsackievirus B3-associated myocardial pathology and viral load reduced by recombinant soluble human decay-accelerating factor in mice. Lab Invest 2003;83:75–85.
[18] Nagaya N, Kangawa K, Itoh T, Iwase T, Murakami S, Miyahara Y, et al. Transplantation of mesenchymal stem cells improves cardiac function in a rat model of dilated cardiomyopathy. Circulation 2005;112:1128–35.

[19] Hanawa H, Abe S, Hayashi M, Yoshida T, Yoshida K, Shiono T, et al. Time course of gene expression in rat experimental autoimmune myocarditis. Clin Sci (Lond) 2002;103:623–32.
[20] Kodama M, Hanawa H, Saeki M, Hosono H, Inomata T, Suzuki K, et al. Rat dilated cardiomyopathy after autoimmune giant cell myocarditis. Circ Res 1994;75:278–84.
[21] Fuse K, Kodama M, Hanawa H, Okura Y, Ito M, Shiono T, et al. Enhanced expression and production of monocyte chemoattractant protein-1 in myocarditis. Clin Exp Immunol 2001;124:346–52.
[22] Rollins BJ. Chemokines. Blood 1997;90:909–28.
[23] Iwamoto M, Osajima A, Tamura M, Suda T, Ota T, Kanegae K, et al. Adrenomedullin inhibits pressure-induced mesangial MCP-1 expression through activation of protein kinase A. J Nephrol 2003;16:673–81.
[24] Wong LY, Cheung BM, Li YY, Tang F. Adrenomedullin is both proinflammatory and antiinflammatory: its effects on gene expression and secretion of cytokines and macrophage migration inhibitory factor in NR8383 macrophage cell line. Endocrinology 2005;146:1321–7.
[25] Kolattukudy PE, Quach T, Bergese S, Breckenridge S, Hensley J, Altschuld R, et al. Myocarditis induced by targeted expression of the MCP-1 gene in murine cardiac muscle. Am J Pathol 1998;152:101–11.
[26] Hippenstiel S, Witzenrath M, Schmeck B, Hocke A, Krisp M, Krull M, et al. Adrenomedullin reduces endothelial hyperpermeability. Circ Res 2002;91:618–25.
[27] Kim W, Moon SO, Sung MJ, Kim SH, Lee S, Kim HJ, et al. Protective effect of adrenomedullin in mannitol-induced apoptosis. Apoptosis 2002;7:527–36.
[28] Tokunaga N, Nagaya N, Shirai M, Tanaka E, Ishibashi-Ueda H, Harada-Shiba M, et al. Adrenomedullin gene transfer induces therapeutic angiogenesis in a rabbit model of chronic hind limb ischemia: benefits of a novel nonviral vector gelatin. Circulation 2004;109:526–31.
[29] Nagaya N, Mori H, Murakami S, Kangawa K, Kitamura S. Adrenomedullin: angiogenesis and gene therapy. Am J Physiol Regul Integr Comp Physiol 2005;288:R1432–7.
[30] Lee JK, Zaidi SH, Liu P, Dawood F, Cheah AY, Wen WH, et al. A serine elastase inhibitor reduces inflammation and fibrosis and preserves cardiac function after experimentally-induced murine myocarditis. Nat Med 1998;4:1383–91.
[31] Ono K, Matsumori A, Shioi T, Furukawa Y, Sasayama S. Contribution of endothelin-1 to myocardial injury in a murine model of myocarditis: acute effects of bosentan an endothelin receptor antagonist. Circulation 1999;100:1823–9.
[32] Tsuruda T, Costello-Boerrigter LC, Burnett JC. Matrix metalloproteinases: pathways of induction by bioactive molecules. Heart Fail Rev 2004;9:53–61.
[33] Plank C, Hartner A, Klanke B, Geissler B, Porst M, Amann K, et al. Adrenomedullin reduces mesangial cell number and glomerular inflammation in experimental mesangioproliferative glomerulonephritis. Kidney Int 2005;68:1086–95.

The Journal of Toxicological Sciences,
Vol.32, No.3, 301-310, 2007

MONITORING OF GENE EXPRESSION IN DIFFERENTIATION OF EMBRYOID BODIES FROM CYNOMOLGUS MONKEY EMBRYONIC STEM CELLS IN THE PRESENCE OF BISPHENOL A

Megumi YAMAMOTO[1,2], Naomi TASE[3], Tsuyoshi OKUNO[4], Yasushi KONDO[4], Suminori AKIBA[5], Nobuhiro SHIMOZAWA[3] and Keiji TERAO[3]

[1]*Physiology Section, Department of Basic Medical Sciences, National Institute for Minamata Disease, 4058-18 Hama, Minamata, Kumamoto 867-0008, Japan*

[2]*Environmental Health Sciences Division, National Institute for Environmental Studies, 16-2 Onogawa, Tsukuba, Ibaraki 305-8506, Japan*

[3]*Tsukuba Primate Research Center, National Institute of Biomedical Innovation, 1-1 Hachimandai, Tsukuba, Ibaraki 305-0843, Japan*

[4]*Advanced Medical Research Laboratories, Tanabe Seiyaku Co., Ltd., 3-16-89 Kashima, Yodogawa-ku, Osaka 532-8505, Japan*

[5]*Department of Epidemiology and Preventive Medicine, Kagoshima University Graduate School of Medical and Dental Sciences, 8-35-1 Sakuragaoka, Kagoshima 890-8544, Japan*

(Received April 24, 2007; Accepted May 8, 2007)

ABSTRACT — An embryonic stem (ES) cell differentiation model would facilitate analysis of developmental processes at the cellular level and the effects of embryotoxic and teratogenic factors *in vitro*. We explored the use of differentiation of embryoid bodies (EBs) from cynomolgus monkey ES cells for embryotoxicity testing. We determined the mRNA expression of various genes using real-time RT-PCR. Oct-3/4 expression was almost completely suppressed on day 14, suggesting that ES cells reached differentiated status in around 14 days. mRNA expression of E-cadherin, connexin 43, caveolin-1, and argininosuccinate synthetase was reproducibly suppressed during EB differentiation in 7–32% of ES cells in three separate experiments. Although these may not be "general stemness marker genes" such as Oct-3/4, they could play a role in readying stem cells for differentiation in response to deletion of signals from feeder cells. Next, we examined the effects of bisphenol A (BPA) on the mRNA expression of several differentiation marker genes for ES cells. That of PAX-6, an ectoderm marker, with 0, 0.1, and 10 μM BPA in 21-day EBs was 3,500%, 6,668%, and 8,394%, respectively, compared with ES cells. The difference between doses of 0 and 10 μM BPA in 21-day EBs was statistically significant ($p=0.049$). Pax-6 activation in the presence of BPA may interfere with the development of eyes, sensory organs, and certain neural and epidermal tissues usually derived from ectodermal tissues. Differentiation of EBs from cynomolgus monkey ES cells could be a useful model for detecting gene expression changes in response to chemical exposure.

KEY WORDS: Embryonic stem cell, Embryoid body, Differentiation, Monkey, Bisphenol A, Embryotoxicity

INTRODUCTION

Embryonic stem (ES) cells have great potential for cell therapy and regenerative medicine, but also represent a dynamic system suitable for identifying potential molecular targets for the development of novel

Correspondence: Megumi YAMAMOTO (E-mail: yamamoto@nimd.go.jp)

drugs, providing an *in vitro* system to examine safety or potential toxicity in humans (Davila *et al.*, 2004; Wobus and Boheler, 2005). Particularly promising is the ES cell differentiation model, which includes developmental processes from early embryonic stages up to terminally differentiated cell types and which would enable us to analyze developmental processes at the cellular level and to determine the effects of embryotoxic and teratogenic factors *in vitro*. Establishing a reliable *in vitro* embryogenesis model would also contribute to a reduction in the number of animal experiments required for medical and pharmacological testing.

Experimental studies using non-human primate ES cells have advantages such as similar characteristics to human ES cells that are not observed in murine ES cells, and avoidance of the ethical problems caused by the use of human ES cells (Thomson *et al.*, 1995; Suemori and Nakatsuji, 2003; Adachi *et al.*, 2006; Byrne *et al.*, 2006). To date, however, the ES cell test for testing embryotoxicity primarily uses murine ES cells (Spielmann *et al.*, 1997; Scholz *et al.*, 1999; Imai and Nakamura, 2006). As a result, our knowledge on the molecular and cellular aspects of ES cells for embryotoxicity testing is based mainly on murine cells, and information on non-human primate ES cells is limited.

In the course of ES cell differentiation, genes encoding tissue-specific proteins are expressed in a developmentally controlled time pattern that closely resembles what is observed during embryogenesis. ES cells differentiate *in vitro* into embryoid bodies (EBs) comprising endoderm, mesoderm and ectoderm cell layers in the absence of the self-renewal signals provided by feeder layers (Weitzer, 2006). EB formation is considered to mimic embryo development during the stages of pre-gastrulation and early gastrulation. Using a mouse EB model, Wartenberg *et al.* examined anti-angiogenic agents in an *in vitro* assay system (Wartenberg *et al.*, 1998). However, to our knowledge, little information is available on the primate EB differentiation model for embryotoxicity screening.

Bisphenol A (BPA) is commonly used in various industries. Its monomer is used for polycarbonate plastic production, and its resin form is used as linings for most food and beverage cans, as dental sealant, and as an additive in other widely used consumer products. BPA is known to elicit weak estrogenic activity in *in vitro* and *in vivo* test systems. Although molecular mechanisms studies have revealed a variety of pathways in which BPA can stimulate cellular responses at very low doses in addition to the effects initiated by its binding to the classical estrogen receptors, there is little information available concerning the effect of BPA on early embryogenesis (vom Saal and Hughes, 2005; Kang *et al.*, 2006).

In the present study, to develop a model system for primate embryotoxicity testing, we used BPA as a model compound and examined changes of gene expression in response to exposure to BPA using cynomolgus monkey EB differentiation. We conducted experiments in three steps. Firstly, we determined the time necessary for EB differentiation in cynomolgus monkey ES cells, examining the expression of Oct-3/4, a POU-class transcription factor. This stemness marker gene was used since loss of pluripotency during spontaneous or induced differentiation has been correlated with progressive loss of Oct-3/4 expression (Niwa, 2001; Mitalipov *et al.*, 2003). In addition to morphological changes, we determined mRNA expression levels using real-time RT-PCR. This quantitative approach is rapid and sensitive and is considered suitable for pharmacological and cytotoxicity screening. Monitoring of ES cell differentiation with quantitative PCR has recently been reported (Noaksson *et al.*, 2005). Secondly, we examined the expression of several genes whose proteins were highly expressed in ES cells compared with EBs. These genes were selected on the basis of preliminary results obtained from a comparison of the protein-expression profiles of various genes in 12–16-day-old CMK-6 ES cells and CMK-6 EBs with Green Fluorescent Protein (Furuya *et al.*, 2003) using Power Blot™, a Western blot array analysis (unpublished result). In the third step, we examined the effects of BPA on mRNA expression of the following differentiation marker genes for ES cells: α-fetoprotein (AFP) and GATA-4 as endoderm markers; BMP-4 and Brachyury as mesoderm markers; and PAX-6 and N-CAM as ectoderm markers.

MATERIALS AND METHODS

Cell culture

The ES cell lines (CMK-6) used in this study were established from blastocysts of the cynomolgus monkey and were kindly provided by Dr Norio Nakatsuji of Kyoto University (Fig. 1A; Suemori *et al.*, 2001).

ES cells were grown on mouse embryonic fibroblast (MEF) feeder cells that were mitotically inactivated by mitomycin C in Dulbecco's Modified Eagle's Medium (DMEM/F12) (SIGMA) supplemented with

20% knock-out serum replacement (Invitrogen), 1% non-essential amino acids (SIGMA) and 2 mM L-glutamine (SIGMA) at 37°C in a humidified 5% CO_2 atmosphere.

For EB differentiation, entire ES cells colonies were loosely detached by 0.1% (w/v) collagenase (Wako Pure Chemical) from the feeder cells and transferred into a feeder-free 25 cm^2 flask (SUMILON) for floating culture. The medium was changed after the first day and half of it was changed every 7 days.

EBs (2×10^5/ml) were incubated for 7, 14 or 21 days with 0.1 μM or 10 μM BPA (SIGMA). In the control group, the same volume of DMSO was added to the media. Stock BPA (100 mM) was dissolved in DMSO and was stored at −20°C. The BPA was further diluted in culture medium just before use, and was sterilized through a filter with a pore size of 0.22 μm. The final DMSO concentration did not exceed 0.1% (vol/vol).

When harvesting ES cells and EBs for mRNA expression analysis, they were washed three times with PBS and then pooled at −80°C until RNA extraction.

Quantitative real-time RT-PCR

Total RNA from ES cells and EBs was isolated using a RNeasy Plus Mini kit (QIAGEN), which includes removal of genomic DNA contamination before cDNA synthesis. Samples were collected from three separate culture experiments.

cDNAs were synthesized from total RNA ranging from 100 ng to 1 μg using QuantiTect Reverse Transcription (QIAGEN) after elimination of genomic DNA contamination.

β-actin and differentially expressed genes were quantitatively detected with a LightCycler Instrument (Roche Diagnostics) using the LightCycler FastStart DNA Mater^{PLUS} SYBR Green I (Roche Diagnostics) according to the manufacturer's instructions.

The primers for each gene were designed and synthesized on the basis of respective information in NCBI or ENSEMBL using the software of Premiere Biosoft, so that the targets were 75–200 bp in length (SIGMA GENOSYS, Table 1).

PCR amplification was performed in a total volume of 20 μl containing cDNA and each primer (0.5 μM). The PCR cycling conditions were 95°C for 10 min followed by 45 cycles of 95°C for 10 sec, 60°C for 10 sec, and 72°C for 15 sec. The fluorescent product at the end of the 72°C extension period was detected. All PCR assays were performed in at least duplicate.

The data obtained were analyzed using the LightCycler analysis software. To confirm the amplification specificity, we subjected the PCR products to melting curve analysis. The results are given as the mean ± SE of samples from three separate culture experiments. The statistical analysis was conducted using Kruskal–Wallis test.

RESULTS

As shown in Fig. 1A and B, cynomolgus monkey ES cells spontaneously differentiated into EBs after separation from the MEFs. Fig. 2 shows the time-course of mRNA expression of Oct-3/4 in EBs in relation to that on Day 1 (ES cell). The average mRNA expression levels of Oct-3/4 in EBs were 3%, 0.9%, and 0.4% at 7 days, 14 days and 21 days, respectively, compared with ES cells. No significant effect of BPA on Oct-3/4 expression in EB differentiation was observed.

Next, we examined the mRNA expression of genes selected by the preliminary experiments

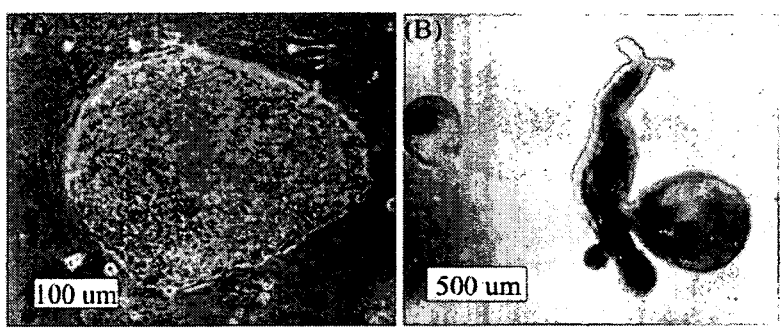

Fig. 1. A: Cynomolgus monkey ES cells, CMK-6.
B: EBs derived from CMK-6 ES cells on Day 14.

described in the Introduction. E-cadherin, connexin 43, caveolin-1, and ASS were consistently suppressed during EB differentiation. In the absence of BPA, the mRNA expression of E-cadherin was suppressed to 12%, 20%, and 21% at 7 days, 14 days and 21 days, respectively, compared with ES cells (Fig. 3A). In the absence of BPA, the mRNA expression of connexin 43 was suppressed to 32%, 32% and 27% at 7 days, 14 days and 21 days, respectively (Fig. 3B). In the absence of BPA, the mRNA expression of caveolin-1 was suppressed to 17%, 26% and 21% at 7 days, 14 days and 21 days, respectively (Fig. 3C). In the absence of BPA, the mRNA expression of ASS was suppressed to 10%, 9% and 7% at 7 days, 14 days and 21 days, respectively (Fig. 3D). There were no detectable differences on microscopy between the BPA treatment and non-treatment groups. In addition, no significant effect of BPA was observed on the expression of these genes in EB differentiation.

In the third step, we examined the effects of BPA on the mRNA expression of the following differentiation marker genes for ES cells: AFP, GATA-4, BMP-4, Brachyury, PAX-6, and N-CAM. The results for two genes, AFP and PAX-6, which gave reproducible results in three separate cultures, are presented in Fig. 4A and B. The mean AFP mRNA expression in 14-day EBs was 204,132% in the presence of 10 μM BPA and 130,635% in the absence of BPA. The difference was

Table 1. Primer sequences for real timeRT-PCR.

Gene	Primers
β-actin	F: ACCCCGTGCTGCTGACC
	R: CCAGAGGCGTACAGGGATAGC
Oct-3/4	F: GCTCCTGAAGCAGAAGAGGATCACC
	R: GCCCTTCTGGCGCCGGTTACAGAAC
E-cadherin	F: AAGACCAAGTGACCACCTTAGAG
	R: AAACAGCAAGAGCAGCAGAATC
Connexin-43	F: TTCAATGGCTGCTCCTCACC
	R: GCTCACTTGCTTGCTTGTTGTA
Caveolin-1	F: CGGCTCAACTCGCATCTCAAG
	R: GCCAGGAACACCGTCAGGA
ASS	F: TGGCTGAAGGAACAAGGCTATG
	R: GCTGACATCCTCAATGAACACC
AFP	F: AGCTTGGTGGTGGATGAA
	R: CAGCCTCAAGTTGTTCCTCT
PAX-6	F: ACAGACACAGCCCTCACAAAC
	R: ATCATAACTCCGCCCATTCACC

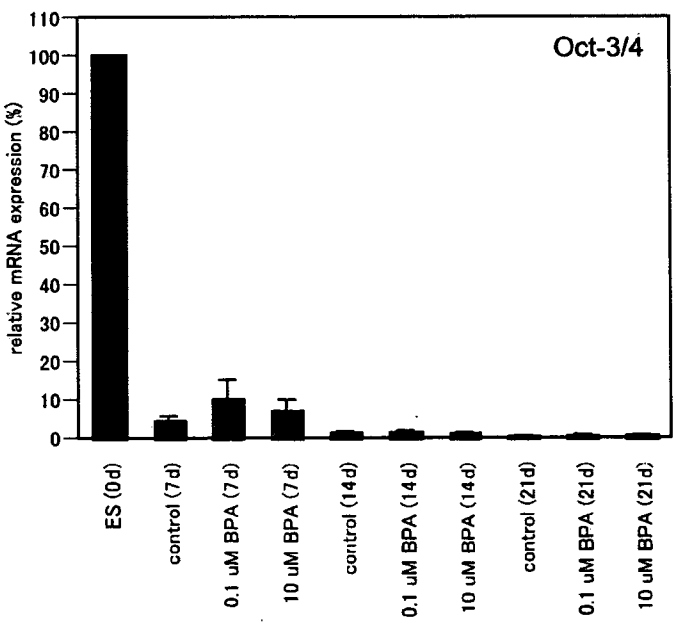

Fig. 2. mRNA expression of Oct-3/4 in EB differentiation at 7, 14 and 21 days. Control: DMSO; 0.1 uM: 0.1 μM BPA; 10 uM: 10 μM BPA. Values are mean ± SE of three independent experiments.

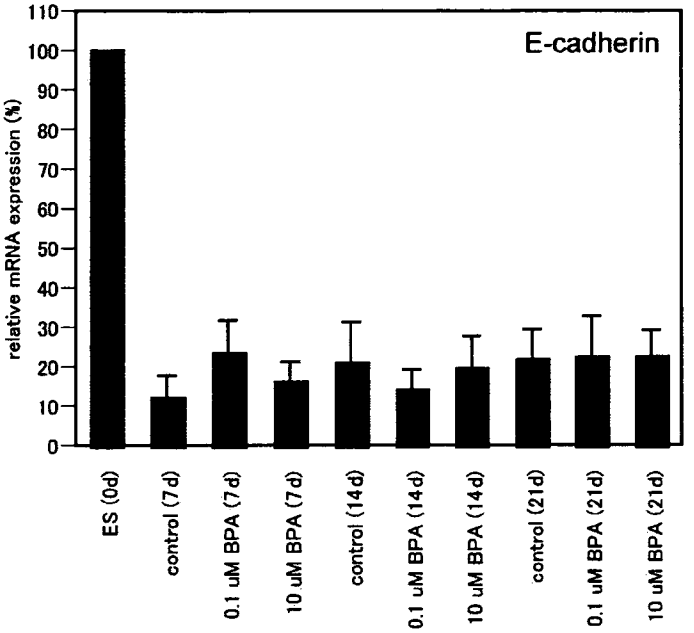

Fig. 3A. mRNA expression of E-cadherin in EB differentiation at 7, 14 and 21 days. Control: DMSO; 0.1 uM: 0.1 μM BPA; 10 uM: 10 μM BPA. Values are mean ± SE of three independent experiments.

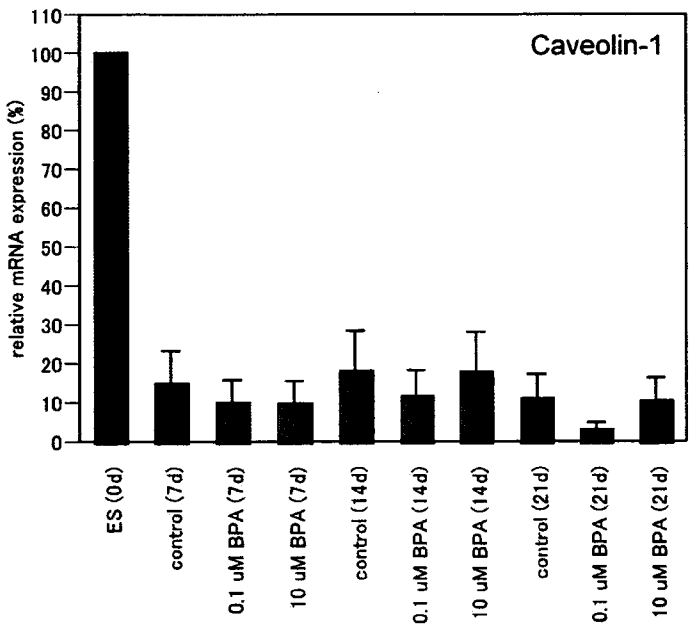

Fig. 3B. mRNA expression of caveolin-1 in EB differentiation at 7, 14 and 21 days. Control: DMSO; 0.1 uM: 0.1 μM BPA; 10 uM: 10 μM BPA. Values are mean ± SE of three independent experiments.

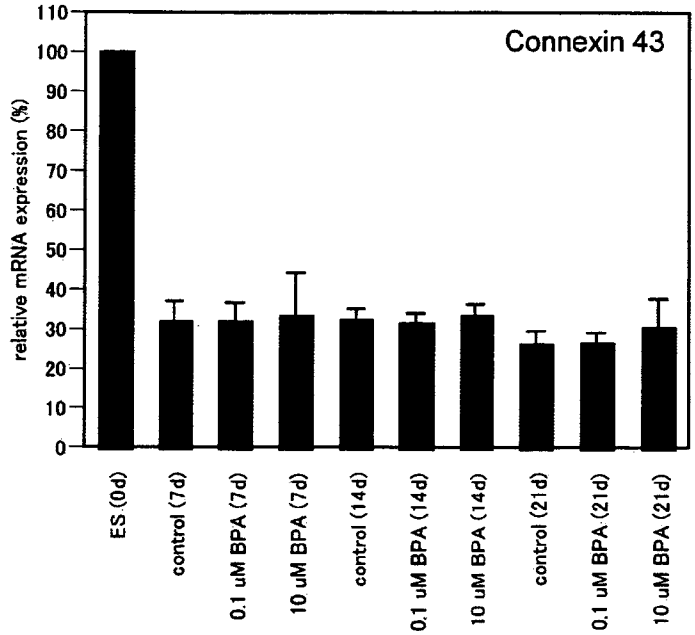

Fig. 3C. mRNA expression of connexin-43 in EB differentiation at 7, 14 and 21 days. Control: DMSO; 0.1 uM: 0.1 μM BPA; 10 uM: 10 μM BPA. Values are mean ± SE of three independent experiments.

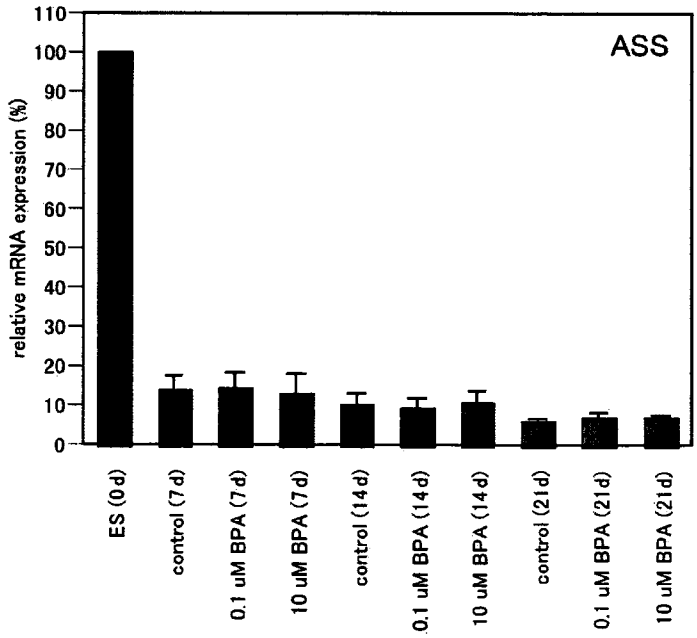

Fig. 3D. mRNA expression of ASS in EB differentiation at 7, 14 and 21 days. Control: DMSO; 0.1 uM: 0.1 μM BPA; 10 uM: 10 μM BPA. Values are mean ± SE of three independent experiments.

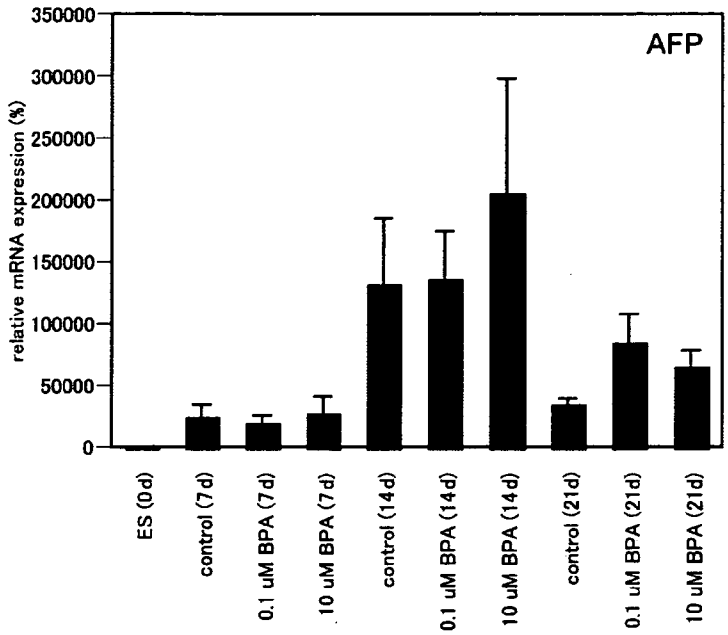

Fig. 4A. Effect of BPA on AFP mRNA expression in EB differentiation at 7, 14 and 21 days. Control: DMSO; 0.1 uM: 0.1 μM BPA; 10 uM: 10 μM BPA. Values are mean ± SE of three independent experiments.

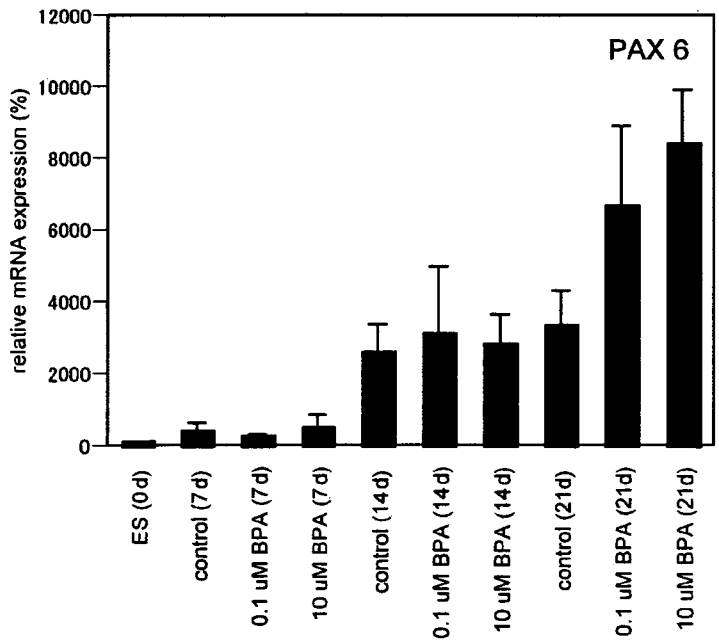

Fig. 4B. Effect of BPA on PAX-6 mRNA expression in EB differentiation at 7, 14 and 21 days. Control: DMSO; 0.1 uM: 0.1 μM BPA; 10 uM: 10 μM BPA. Values are mean ± SE of three independent experiments.

not statistically significant (p=0.513). In 21-day EBs, the average mRNA expression in the presence of 0, 0.1 μM and 10 μM was 33,418% (reference category for p-value calculation), 80,100% (p=0.049) and 63,787% (p=0.049) respectively. The averages of three separate experiments of PAX-6 mRNA expression in the presence of 0, 0.1 and 10 μM BPA in 21-day EBs were 3,500%, 6,668% and 8,394%, respectively, compared with ES cells. The difference between doses of 0 and 10 μM was statistically significant (p=0.049). The difference between doses of 0 and 0.1 μM was not statistically significant (p=0.275). On Days 7 and 14, BPA did not show any evident effects on PAX-6 mRNA expression.

DISCUSSION

mRNA expression of Oct-3/4 was almost completely suppressed on Day 14, suggesting that ES cells reached differentiated status in around 14 days. E-cadherin, connexin 43, caveolin-1 and ASS were also consistently suppressed during EB differentiation (Table 2). The time patterns of their mRNA expression were similar to that of Oct-3/4. The cadherins are a class of transmembrane proteins that play important roles in cell adhesion. E-cadherin is first expressed in the 2-cell stage of mammalian development, and becomes phosphorylated in the 8-cell stage, where it causes compaction (Halbleib and Nelson, 2006). Connexin 43 is known to be related to gap junction-related protein, and gap junctions play significant regulatory roles in embryonic development (King and Lampe, 2005). Caveolin-1 has been shown to be the structural protein of plasmalemmal invaginations, termed caveolae, and functions as a tumor suppressor gene (Sotgia *et al.*, 2006). The tyrosine-phosphorylated form of caveolin-1 co-localizes with focal adhesions, suggesting that caveolin-1 plays a role in migration. Down-regulation of caveolin-1 leads to less efficient migration *in vitro*. ASS is an enzyme that catalyzes argininosuccinate synthesis from citrulline and aspartate, and is responsible for the third step of the urea cycle and one of the reactions of the citrulline-NO cycle (Husson *et al.*, 2003). ASS is highly conserved from bacteria to humans, and is present in large amounts in many tissues, including liver and kidney. It is difficult to discuss the significance of down-regulation of E-cadherin, connexin 43, caveolin-1, and ASS during EB differentiation, because they were selected by their ES/EB ratio in protein expression profiling. They may not be "general stemness marker genes" such as Oct-3/4, expression of which is always suppressed in any type of differentiation. However, they at least play a role, not only in maintaining the undifferentiated stem cell state, but also in readying stem cells for EB differentiation in response to deletion of signals from the MEFs. Reproducible results in some genes were obtained in separate experiments, indicating that this EB differentiation system could work as an embryotoxicity test.

Table 2. Average of mRNA expression of undifferentiated stem cell state-related genes.

	1d-ES	7d-EB	14d-EB	21d-EB
Oct-3/4	100%	3%	0.9%	0.4%
E-cadherin	100%	12%	20%	21%
Connexin 43	100%	32%	32%	27%
Caveolin-1	100%	17%	26%	21%
ASS	100%	10%	9%	7%

In response to BPA, expression of AFP andPAX-6 was increased at least temporarily. AFP is a glycoprotein that is produced principally in the fetal liver and gastrointestinal tract and is temporarily present during embryonic development. Estrogens were reported to modify AFP, exhibiting growth-suppressive properties (Vakharia and Mizejewski, 2000). BPA may interfere with the interaction between AFP and estrogen in EB differentiation. Recently, non-estrogenic effects of BPA on the central nervous system have been reported. In mice, prenatal and neonatal exposure to BPA induces a significant increase in the levels of dopamine D_1 receptor mRNA in the brain and increases central dopamine D_1 receptor-mediated activity (Suzuki *et al.*, 2003). In addition, expression of PAX-6 mRNA in embryos of *Xenopus laevis* was reported to be suppressed by treatment with 50 or 100 μM BPA from stage 10.5 to stage 35 (Imaoka *et al.*, 2007). PAX-6 is recognized as a master control gene for the development of eyes, sensory organs and certain neural and epidermal tissues that are usually derived from ectodermal tissues (Kondoh *et al.*, 2004). BPA may be related to one of the above functions in early development. The reason why the mRNA expression results for some genes were not reproducible may be that inappropriate primers were used for RT-PCR, that transfection with GFP may alter the characteristics of cells or that changes due to BPA may have occurred at the translational level rather than the transcriptional level.

In conclusion, our results indicated that this EB differentiation from cynomolgus monkey ES cells could work for detecting changes of gene expression in

response to BPA exposure, and could contribute to developing a primate ES embryotoxicity test in the near future.

ACKNOWLEDGMENT

The authors are grateful to Dr Colin R. Jefcoate (University of Wisconsin-Madison, USA), Dr Seishiro Hirano (National Institute for Environmental Studies), Dr Kunihiko Nakamura (National Institute for Minamata Disease) and Dr Koji Arizono (Prefectural University of Kumamoto) for their valuable comments, and to Ms Tomoyo Aratake and Ms Kiyoko Iwatsubo (National Institute for Minamata Disease) for their assistance in preparing the manuscript. This study was partly supported by a Grant (No. H16- REGENERATION-002) from the Ministry of Health, Labour, and Welfare of Japan.

REFERENCES

Adachi, K., Kawase, E., Yasuchika, K., Sumi, T., Nakatsuji, N. and Suemori, H. (2006): Establishment of the gene-inducible system in primate embryonic stem cell lines. Stem Cells, **24**, 2566-2572.

Byrne, J.A., Mitalipov, S.M., Clepper, L. and Wolf, D.P. (2006): Transcriptional profiling of rhesus monkey embryonic stem cells. Biol. Reprod., **75**, 908-915.

Davila, J.C., Cezar, G.G., Thiede, M., Strom, S., Miki, T. and Trosko, J. (2004): Use and application of stem cells in toxicology. Toxicol. Sci., **79**, 214-223.

Furuya, M., Yasuchika, K., Mizutani, K., Yoshimura, Y., Nakatsuji, N. and Suemori, H. (2003): Electroporation of cynomolgus monkey embryonic stem cells. Genesis, **37**, 180-187.

Halbleib, J.M. and Nelson, W.J. (2006): Cadherins in development: Cell adhesion, sorting, and tissue morphogenesis. Gene Dev., **20**, 3199-3214.

Husson, A., Brasse-Lagnel, C., Fairand, A., Renouf, S. and Lavoinne, A. (2003): Argininosuccinate synthetase from the urea cycle to the citrulline-NO cycle. Eur. J. Biochem., **270**, 1887-1899.

Imai, K. and Nakamura, M. (2006): *In vitro* embryotoxicity testing of metals for dental use by differentiation of embryonic stem cell test. Congenit Anom., **46**, 34-38.

Imaoka, S., Mori, T. and Kinoshita, T. (2007): Bisphenol A causes malformation of the head region in embryos of Xenopus laevis and decreases the expression of the ESR-1 gene mediated by Notch signaling. Biol. Pharm. Bull., **30**, 371-374.

Kang, J.H., Kondo, F. and Katayama, Y. (2006): Human exposure to bisphenol A. Toxicology, **226**, 79-89.

King, T.J. and Lampe, P.D. (2005): Temporal regulation of connexin phosphorylation in embryonic and adult tissues. Biochim. Biophys. Acta, **1719**, 24-35.

Kondoh, H., Uchikawa, M. and Kamachi, Y. (2004): Interplay of Pax6 and SOX2 in lens development as a paradigm of genetic switch mechanisms for cell differentiation. Int. J. Dev. Biol., **48**, 819-827.

Mitalipov, S.M., Kuo, H.C., Hennebold, J.D. and Wolf, D.P. (2003): Oct-4 expression in pluripotent cells of the rhesus monkey. Biol. Reprod., **69**, 1785-1792.

Niwa, H. (2001): Molecular mechanism to maintain stem cell renewal of ES cells. Cell Struct. Funct., **26**, 137-148.

Noaksson, K., Zoric, N., Zeng, X., Rao, M.S., Hyllner, J., Semb, H., Kubista, M. and Sartipy, P. (2005): Monitoring differentiation of human embryonic stem cells using real-time PCR. Stem Cells, **23**, 1460-1467.

Scholz, G., Pohl, I., Genschow, E., Klemm, M. and Spielmann, H. (1999): Embryotoxicity screening using embryonic stem cells *in vitro*: Correlation to *in vivo* teratogenicity. Cells Tissues Organs, **165**, 203-211.

Sotgia, F., Rui, H., Bonuccelli, G., Mercier, I., Pestell, R.G. and Lisanti, M.P. (2006): Caveolin-1, mammary stem cells, and estrogen-dependent breast cancers. Cancer Res., **66**, 10647-10651.

Spielmann, H., Pohl, I., Doering, B., Liebsch, M. and Moldenhauer, F. (1997): The embryonic stem cell test, an *in vitro* embryotoxicity test of two permanent mouse cell lines: 3t3 fibroblasts and embryonic stem cells. In Vitro Toxicol., **10**, 199-207.

Suemori, H., Tada, T., Torii, R., Hosoi, Y., Kobayashi, K., Imahie, H., Kondo, Y., Iritani, A. and Nakatsuji, N. (2001): Establishment of embryonic stem cell lines from cynomolgus monkey blastocysts produced by IVF or ICSI. Dev. Dynam., **222**, 273-279.

Suemori, H. and Nakatsuji, N. (2003): Growth and differentiation of cynomolgus monkey ES cells.

Method Enzymol., **365**, 419-429.

Suzuki, T., Mizuo, K., Nakazawa, H., Funae, Y., Fushiki, S., Fukushima, S., Shirai, T. and Narita, M. (2003): Prenatal and neonatal exposure to bisphenol-A enhances the central dopamine D1 receptor-mediated action in mice: Enhancement of the methamphetamine-induced abuse state. Neuroscience, **117**, 639-644.

Thomson, J.A., Kalishman, J., Golos, T.G., Durning, M., Harris, C.P., Becker, R.A. and Hearn, J.P. (1995): Isolation of a primate embryonic stem cell line. P. Natl. Acad. Sci. U. S. A., **92**, 7844-7848.

Vakharia, D. and Mizejewski, G.J. (2000): Human alpha-fetoprotein peptides bind estrogen receptor and estradiol, and suppress breast cancer. Breast Cancer Res. Tr., **63**, 41-52.

vom Saal, F.S. and Hughes, C. (2005): An extensive new literature concerning low-dose effects of bisphenol A shows the need for a new risk assessment. Environ. Health Persp., **113**, 926-933.

Wartenberg, M., Gunther, J., Hescheler, J. and Sauer, H. (1998): The embryoid body as a novel *in vitro* assay system for antiangiogenic agents. Lab. Invest., **78**, 1301-1314.

Weitzer, G. (2006): Embryonic stem cell-derived embryoid bodies: An *in vitro* model of eutherian pregastrulation development and early gastrulation. Handb. Exp. Pharmacol., **174**, 21-51.

Wobus, A.M. and Boheler, K.R. (2005): Embryonic stem cells: Prospects for developmental biology and cell therapy. Physiol. Rev., **85**, 635-678.

[Full Paper]

The protein expression profile of cynomolgus monkey embryonic stem cells in two-dimensional gel electrophoresis: a successful identification of multiple proteins using human databases

Masako Nakahara[1], Kumiko Saeki[1], Yoshiko Yogiashi[1], Akiko Kimura[1], Akiko Horiuchi[1], Naoko Nakamura[1], Asako Yoneda[1], Koichi Saeki[1], Satoko Matsuyama[1], Megumi Nakamura[2], Tosifusa Toda[2], Yasushi Kondo[3], Yasushi Kaburagi[4] and Akira Yuo[1]

SUMMARY

Global gene and protein expression analyses have had great impacts on scientific progresses in this new era of bioinformatics. Although studies using murine and human materials can fully exploit the large volume of their databases, there are quite a few inconveniences for an investigation on non-human primate materials due to still insufficient data collections. Here we examined the availability of human databases for the protein identification process using the two-dimensional electrophoresis-based proteomic study in cynomolgus monkey embryonic stem (ES) cells. Querying public human protein databases, we successfully identified multiple protein spots via mass spectrometric analysis using MALDI-TOF apparatus. The results of the protein identification were confirmed by western blotting using polyclonal antibodies raised against human epitopes. Interestingly, the results of western blotting further identified the existence of previously unreported multiple isoforms of common proteins including glycolytic pathway enzymes. Thus, combined analyses of the mass spectrometry querying the *Homo sapience* databases and the western blotting using polyclonal antibodies is highly effective in determining protein expressions in monkey cells. Our success in obtaining a draft protein expression profile of cynomolgus monkey ES cells will contribute to the promotion of non-human primate ES cell researches.

Key words: cynomolgus monkey, embryonic stem cells, proteomics, two-dimensional electrophoresis, mass spectrometric analysis.

INTRODUCTION

Recent years, researches on non-human primates are of growing importance in the fields of life science. It has been emphasized that animal studies with clinical concerns such as a toxicological study of environmental factors and safety evaluation of newly invented drugs should be performed using primate, but not rodent, models. Although studies using rodents are feasible in technical and economical points of view, they do not always provide sufficient informations applicable to human cases. The differences in metabolism and tissue sensitivity of the drug between

[1] Department of Hematology, Research Institute, International Medical Center of Japan, Tokyo, Japan.
[2] Research Team for Molecular Biomarkers, Tokyo Metropolitan Institute of Gerontology, Tokyo, Japan.
[3] Advanced Medical Research Laboratories, Tanabe Seiyaku Co. Ltd., Osaka, Japan.
[4] Department of Metabolic Disorder, Research Institute, International Medical Center of Japan, Tokyo, Japan.
Correspondence address: Akira Yuo; Department of Hematology, Research Institute, International Medical Center of Japan, 1-21-1, Toyama, Shinjuku-ku, Tokyo 162-8655, Japan.

Abbreviations: ES, embryonic stem; 2-DE, two-dimensional gel electrophoresis; MEF, murine embryonic fibroblast; MMC, mitomycin C; SDS, sodium dodecyl sulphate; PMF, peptide mass fingerprinting; HSP60, 60-kDa heat shock protein; HSC70, heat shock cognate 71-kDa protein; TIM, triosephosphate isomerase; GAPDH, glyceraldehyde-3-phosphate dehydrogenase; VDAC-1, voltage-dependent anion-selective channel protein 1; PKM2, pyruvate kinase isozyme M2; PGK1, phosphoglycerate kinase 1.

(Received October 16, 2006, Accepted December 22, 2006, Published March 15, 2007)

rodents and primates are not negligible. In addition, the short lifetime of rodents cannot afford the longtime, chronic effect of drugs. The primate study is also essential to understand the molecular mechanism of diseases. An integrated study on genome, transcriptome or proteome, which has become a powerful tool to elucidate the complicated mechanisms of human multi-factorial diseases, should better be performed using primate, but not rodent, models. Indeed, growing numbers of pedigrees of cynomolgus monkeys that provide excellent models for human diseases have been prepared[1, 2].

In addition to the living individuals, cell lines established from monkey tissues play beneficial roles. For example, embryonic stem (ES) cells, which are a valuable resource in regenerative medicine because of their high capacity to differentiate into a broad range of cell types, have particularly large impacts. It is known that primate ES cells show different characteristics from murine ES cells: they have different extracellular and intracellular signaling pathways for the maintenance of pluripotency[3] and distinctive differentiation capacities[4]. Thus, the promotion of researches on primate ES cells is now becoming exceedingly important. Although studies using human ES cells are essential for clinical application, basic researches using monkey ES cells still have importance because they can provide good allotransplantation models required for pre-clinical studies[5, 6]. Moreover, ethical regulation that is heavily imposed on the usage of human ES cells is remissive concerning the use of monkey ES cells. Thus biotechnological manipulation, including gene transfer, can immediately be applied to the usage of monkey ES cells, which will contribute to the further advance in our understanding of human ES cells.

Despite an increasing requirement to promote the monkey ES cell study, construction of integrated bioinformatics on non-human primates is still underway, and only a small volume of individually collected data is available at present. As a result, we often experience difficulties in constructing monkey polymerase chain reaction primers and the primers designed from human databases do not necessarily work in monkey samples. As compared with the informations on genes or messages, data on proteins are rather compressed due to three-to-one correspondence, where a train of three nucleotides corresponds to one amino acid and the last nucleotide in each train has a large redundancy. In addition, degrees of freedom in amino acid sequence are lower than those in nucleotide sequences due to functional requirement of proteins. Thus, in contrast to the genomic and transcriptomic studies, proteomic analysis of monkey samples might be effectively achieved querying human databases.

In the present study, we successfully determined a protein expression profile using the two-dimensional gel electrophoresis (2-DE) and human proteome databases in undifferentiated cynomolgus monkey ES cells. Our results will encourage the promotion of the monkey proteome study in the present situation, without waiting for the future accomplishment of the data construction of monkey bioinformatics.

MATERIALS AND METHODS

1. Cells culture

Murine embryonic fibroblasts (MEFs), which had been treated with Dulbecco's modified Eagle's medium containing mitomycin C (MMC) for 3 hours, were seeded on the dishes coated with 0.1% gelatin. Cynomolgus monkey ES cells[7] were maintained on MMC-treated MEF-coated dishes in DMEM/F12 medium supplemented with 20% heat inactivated fetal bovine serum, 8 ng/ml fibroblast growth factor 2, 10 ng/ml recombinant human bone morphogenic protein 4, 1 mM β-mercaptoethanol, 1 mM L-glutamine, 10 U/ml penicillin and 10 μg/ml streptomycin. Monkey ES cells were passaged every 2 days using 0.25% trypsin treatment for one minutes and were seeded at split ratios of 1:2 to 1:4 on new MEF-coated dishes. For the collection of ES cells for 2-DE, ES cells were detached by 0.2% EDTA treatment to avoid the contamination of MEFs.

2. Two-dimensional gel electrophoresis (2-DE)

ES cells were collected by 0.2% EDTA treatment. After washing the cells with washing buffer (10 mM Tris-HCl buffer, pH 8.0, 5 mM magnesium acetate), 4×10^7 cells were suspended with 7 volumes of lysis buffer containing 2 M thiourea, 7 M urea, 4% (w/v) CHAPS and 1 mM Pefablc SC PLUS (Roche Diagnostics GmbH, Mannheim, Germany). The cell suspensions were kept for 10 minutes on ice, sonicated intermittently and centrifuged at 12,000 g for 10 minutes at 4°C, and then the supernatant fractions were collected. The protein concentration was determined in the lysis solution with a dye reagent from Amersham Biosciences using bovine serum albumin as a standard. The lysate was alkylated with Ready Prep™ Reduction-Alkylation Kit (Bio Rad Laboratories, Hercules, CA). The 120 μg protein lysate per gel were subjected to 2-DE. The first-dimensional isoelectric focusing was carried out using Immobiline dry strip (18-cm long, pH 3–10 non-linear or pH 6–11 linear) in a horizontal electrophoresis system, Ettan IPGphor (Amersham Biosciences) according to the manufacturer's instructions. After the first dimensional elecrofocusing, IPG gels were equilibrated with buffer containing 50 mM Tris-HCl (pH 8.8), 6 M urea, 30% (v/v) glycerol, 2% (w/v) sodium dodecyl sulphate (SDS), 0.01% BPB and 0.5% dithiothreitol, followed by alkylation with equilibration buffer containing 4.5% idoacetamide instead of 0.5% dithiothreitol at room temperature for 15 minutes. The gels were subjected to the second-dimensional SDS polyacrylamide gel electrophoresis (10% SDS). Proteins were visualized in the gels by staining with SYPRO Ruby Protein Gel Stain (Bio Rad) for overnight. The florescence intensity of each protein spot was digitally recorded by

FluorImager 595 using Image QuaNT software and the protein expression was analyzed by PDQuest software.

3. Mass spectrometric analysis

The mass spectrometric analysis was performed according to the method reported previously[8] with minor modifications. Briefly, each protein spot in SYPRO Ruby-stained gels was picked by FluoroPhoreStar 3000 (Anatech, Tokyo, Japan). The pieces of gels were dehydrated in 50% acetonitrile and 50% ammonium bicarbonate, and then in 100% acetonitrile, and dried up. The proteins were digested with 5 μg/ml trypsin at 30°C. After the overnight protein digestion, peptide fragments in the digest were subjected to MALDI-TOF mass spectrometer (AXIMA-CFR, Shimazdu Corp., Kyoto, Japan) for peptide mass fingerprinting (PMF). Protein identification process was accomplished by a two-tiered approach using Mascot server (Matrix Science Ltd., Franklin St., Boston, MA) for selection of protein candidates and then using Protein Prospector (UCSF Mass Spectrometry Facility, San Francisco, CA) for its verification. In the former, molecular weights and pI values were taken into account as well as % coverage values during candidate protein selection. In the latter, verification was performed using MS-Digest software under a criterion that more than eight m/z values were detected in major peaks of PMF. The activated parameters used in Mascot server query were as follows: primate database of SWISS-PROT and NCBInr, peptide tolerance ±0.4 Da or ±1.0 Da, one missed cleavage and carbamidomethyl modification of cysteine. During MS-Digest software query, acetylation of N-terminal end or lysine and phosphorylation of serine, threonine or tyrosine was considered. Protein identification was repeated at least once with spots from different gels.

4. Two-dimensional Western blotting

The SYPRO Ruby-stained proteins on gels were resolubilized and transferred according to our previously reported method[9]. Briefly, the stained gel was incubated in resolubilization buffer (0.2% w/v SDS, 0.3% w/v Tris, 0.7% w/v glycine) for 10 minutes and mounted onto a PVDF membrane in a semi-dry blotting apparatus (Bio Rad). Electrotransfer was carried out at 4 V/cm^2 for one hour at room temperature using buffer containing 0.3% (w/v) Tris, 1.5% (w/v) glycine, 0.1% (w/v) SDS. The fluorescence images of the blotted PVDF membranes were scanned and recorded by FluorImager 595. The PVDF membranes were further subjected to the immunoblotting using polyclonal antibodies against 60-kDa heat shock protein (HSP60), annexin A5, heat shock cognate 71-kDa protein (HSC70), triosephosphate isomerase (TIM), 14-3-3 proteins, α-enolase, glyceraldehyde-3-phosphate dehydrogenase (GAPDH) (Santa Cruz Biotechnology Inc.), annexin A2 (Abnova Corp., Taipei, Taiwan), voltage-dependent anion-selective channel protein 1(VDAC-1) (Abcam plc., Cambridge, UK), pyruvate kinase isozyme M2 (PKM2), phosphoglycerate kinase 1 (PGK1), serine/threonine-protein kinase 13 (Aurora-C) (Abgent Inc. San Diego, CA), nucleolin, thioredoxin reductase and GTP-binding nuclear protein Ran (Santa Cruz Biotechnology).

RESULTS AND DISCUSSION

While the routine cell passage procedure was performed detaching ES cells by trypsinization, we collected the ES cells by EDTA treatment to prepare 2-DE samples to exclude the contamination by MEFs. The typical 2-DE protein expression patterns of "ES cells" using strips of pH 3–10 and pH 6–11 were shown in Figs. 1A and 1B, respec-

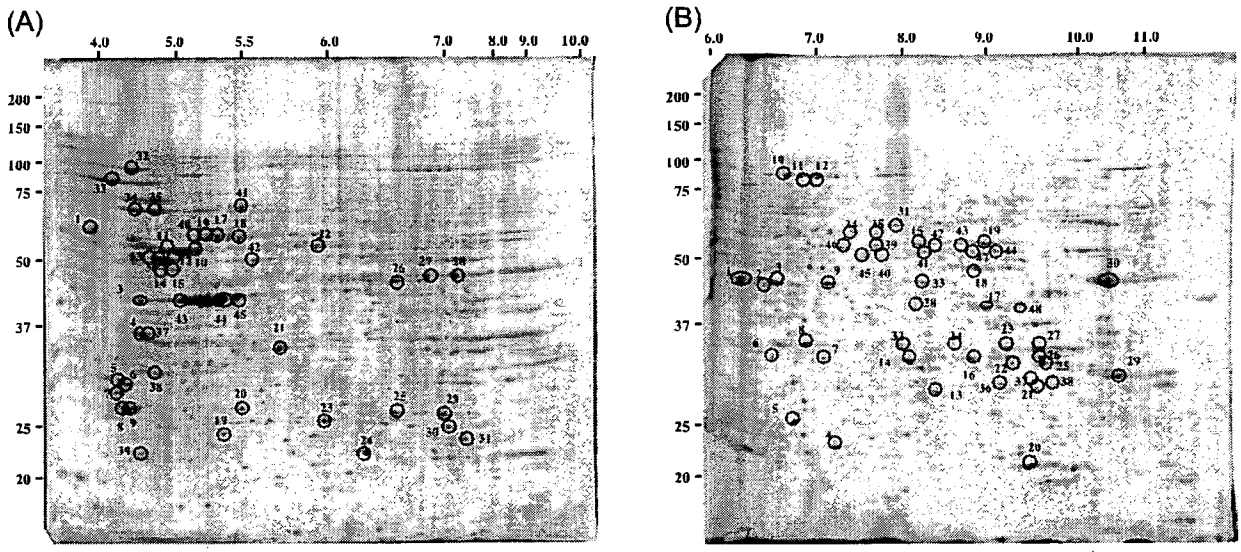

Fig. 1. Protein expression patterns of cynomolgus monkey ES cells in 2-DE.

The SYPRO Ruby staining patterns in the 2-DE using a strip of pH 3–10 non-linear (A) and a strip of pH 6–11 (B) in the first-dimensional isoelectric focusing. A typical result from four independent experiments for each was shown.

Table 1. Identification of the proteins detected in 2-DE gel using a pH 3-10 strip

#	protein name	ID method	mass tolerance	% Coverage	Acc No	Funtion (as listed in Swiss-Prot)
1	calreticulin	MALDI	1	21	P27797	calcium binding chaperone
2	14-3-3 protein ζ	WB			P63104	Adapter protein
3	40S ribosomal protein SA	MALDI	0.4	18	P08865	unknown
4	nucleophosmin	MALDI	0.4	11	P06748	assembly and/or transport of ribosome.
5	tropomyosin-4	MALDI, WB	0.4	11	P67936	stabilizing cytoskeleton actin filaments
6	tropomyosin α-3	MALDI, WB	1	33	P06753	stabilizing cytoskeleton actin filaments
7	14-3-3 protein ε	MALDI, WB	0.4	24	P62258	Adapter protein
8	14-3-3 protein ζ	MALDI, WB	0.4	22	P63104	Adapter protein
9	14-3-3 protein ζ	MALDI, WB	0.4	22	P63104	Adapter protein
10	tublin α ubiquitous	MALDI	0.4	29	P68363	major constituent of microtubules
11	vimentin	MALDI	1	17	P08670	class-III intermediate filaments
12	tublin β-2 chain	MALDI	0.4	11	P07437	the major constituent of microtubules
13	zinc-finger FYVE domain-containing protein 19	MALDI	1	10	Q96K21	unknown
14	ATP synthase β chain	MALDI	0.4	12	P06576	Produces ATP from ADP
15	ATP synthase β chain	MALDI	0.4	12	P06576	Produces ATP from ADP
16	60-kDa heat shock protein (HSP60)	MALDI, WB	0.4	13	P10809	mitochondrial protein import and macromolecular assembly
17	60-kDa heat shock protein (HSP60)	MALDI, WB	0.4	13	P10809	mitochondrial protein import and macromolecular assembly
18	T-complex protein 1 subunit ε	MALDI	0.4	20	P48643	Molecular chaperone
19	ubiquitin carbonyl-terminal hydrolase isozyme	MALDI	1	15	P09936	Ubiquitin-protein hydrolase
20	prohibitin	MALDI	1	28	P35232	DNA synthesis inhibitor
21	L-lactate dehydrogenase B chain	MALDI	0.4	23	P07195	CATALYTIC ACTIVITY: (S)-lactate+NAD+=pyruvate+NADH.
22	protein disulfide-isomerase A3 precursor	MALDI	0.4	22	P30101	Catalyzes the rearrangement of -S-S- bonds
23	peroxiredoxin 6	MALDI	0.4	21	P30041	redox regulation of the cell
24	glutathione S-transferase π	MALDI	0.4	48	P09211	Conjugation of reduced glutathione
25	phosphoglycerate mutase	MALDI	0.4	20	P18669	Interconversion of 3- and 2-phosphoglycerate with 2,3-bisphosphoglycerate
26	elongation factor 1-γ	MALDI	0.4	13	P26641	Probably plays a role in anchoring the complex to other cellular components
27	α-enolase	MALDI, WB	0.4	29	P06733	Multifunctional enzyme that, as well as its role in glycolysis
28	α-enolase	MALDI, WB	0.4	50	P06733	Multifunctional enzyme that, as well as its role in glycolysis
29	phosphoglycerate mutase	MALDI	0.4	30	P18669	Interconversion of 3- and 2-phosphoglycerate with 2,3-bisphosphoglycerate
30	triosephosphate isomerase	MALDI, WB	0.4	29	P60174	CATALYTIC ACTIVITY: D-glyceraldehyde 3-phosphate=glycerone phosphate
31	GTP-binding nuclear protein Ran	MALDI, WB	1	37	P62826	GTP-binding protein involved in nucleocytoplasmic transport
32	nucleolin	MALDI, WB	0.4	13	P19338	It induces chromatin decondensation by binding to histone H1
33	thioredoxin reductase	MALDI, WB	1	16	Q16881	CATALYTIC ACTIVITY: thioredoxin+NADP+=thioredoxin disulfide+NADPH
34	heat shock cognate 71-kDa protein (HSC70)	MALDI, WB	0.4	17	P11142	Chaperone
35	heat shock cognate 71-kDa protein (HSC70)	MALDI, WB	0.4	17	P11142	Chaperone
36	tublin β-2 chain	MALDI	0.4	17	P07437	the major constituent of microtubules
37	annexin A5	MALDI, WB	1	24	P08758	an anticoagulant protein
38	annexin A5	MALDI, WB	1	24	P08758	an anticoagulant protein
39	annexin A5	MALDI, WB	1	24	P08758	an anticoagulant protein
40	60-kDa heat shock protein (HSP60)	MALDI, WB	0.4	13	P10809	mitochondrial protein import and macromolecular assembly
41	zinc-finger protein 192	MALDI	1	6	Q15776	May be involved in transcriptional regulation
42	pigment epithelium-derived factor	MALDI	1	14	P36955	Neurotrophic protein
43	actin cytoplasmic 1	MALDI	0.4	19	P60709	involved in various types of cell motility
44	actin cytoplasmic 1	MALDI	0.4	19	P60709	involved in various types of cell motility
45	actin cytoplasmic 1	MALDI	0.4	19	P60709	involved in various types of cell motility

The protein name listed in UniProt (SwissProt), identification method (ID method), mass tolerance used as activated parameter during MASCOT sever query, percent of the coverage (% coverage), accession number of the protein (Acc No), and function of the protein listed in UniProt (SwissProt) were shown.

Table 2. Identification of the proteins detected in 2-DE gel using a pH 6–11 strip

#	protein name	ID method	mass tolerance	% Coverage	Acc No	Funtion (as listed in Swiss-Prot)
1	α-enolase	WB			P06733	Multifunctional enzyme that, as well as its role in glycolysis
2	α-enolase	WB			P06733	Multifunctional enzyme that, as well as its role in glycolysis
3	α-enolase	MALDI, WB	0.4	23	P06733	Multifunctional enzyme that, as well as its role in glycolysis
4	GTP-binding nuclear protein Ran	MALDI, WB	0.4	28	P62826	GTP-binding protein involved in nucleocytoplasmic transport
5	phosphoglycerate mutase	MALDI, WB	0.4	30	P18669	Interconversion of 3- and 2-phosphoglycerate with 2,3-bisphosphoglycerate
6	annexin A2	WB			P07355	Calcium-regulated membrane-binding protein
7	annexin A2	WB			P07355	Calcium-regulated membrane-binding protein
8	septin 9	MALDI	0.4	18	Q9UHD8	Involved in cytokinesis
9	α-enolase	MALDI, WB	0.4	23	P06733	Multifunctional enzyme that, as well as its role in glycolysis
10	elongation factor 2	MALDI	0.4	13	P13639	promotes GTP-dependent translocation
11	elongation factor 2	MALDI	0.4	13	P13639	promotes GTP-dependent translocation
12	elongation factor 2	MALDI	0.4	13	P13639	promotes GTP-dependent translocation
13	guanine mucleotide-binding protein β-subunit 2-like 1	MALDI	0.4	11	P63244	an intracellular receptor to anchor the activated PKC to the cytoskeleton
14	annexin A2	MALDI, WB	0.4	38	P07355	Calcium-regulated membrane-binding protein
15	pyruvate kinase isozyme M2 (PKM2)	MALDI, WB	1	16	P14618	CATALYTIC ACTIVITY: ATP+pyruvate=ADP+phosphoenolpyruvate.
16	annexin A2	MALDI, WB	0.4	38	P07355	Calcium-regulated membrane-binding protein
17	phosphoglycerate kinase 1 (PGK1)	MALDI, WB	1	33	P00558	glycolytic enzyme, polymerase alpha cofactor protein
18	ATP synthase alpha chain, mitochondrial precursor	MALDI	1	14	P25705	Produces ATP from ADP in the presence of a proton gradient across the membrane
19	pyruvate kinase isozyme M2 (PKM2)	MALDI, WB	1	23	P14618	CATALYTIC ACTIVITY: ATP+pyruvate=ADP+phosphoenolpyruvate.
20	peroxiredoxin-1	MALDI	0.4	25	Q06830	Involved in redox regulation of the cell
21	voltage-dependent anion-selective channel protein 1 (VDAC-1)	MALDI, WB	1	33	P21796	Forms a channel through the mitochondrial outer membrane and also the plasma membrane.
22	transcription elongation factor A protein 2	MALDI	1	18	Q15560	Necessary for efficient RNA polymerase II transcription elongation
23	glyceraldehyde-3-phosphate dehydrogenase (GAPDH)	WB			P04406	CATALYTIC ACTIVITY: D-glyceraldehyde 3-phosphate+phosphate+NAD^-=3-phospho-D-glyceroyl phosphate+NADH.
24	glyceraldehyde-3-phosphate dehydrogenase (GAPDH)	WB			P04406	CATALYTIC ACTIVITY: D-glyceraldehyde 3-phosphate+phosphate+NAD^-=3-phospho-D-glyceroyl phosphate+NADH.
25	paired box protein pax-8	MALDI	0.4	17	Q06710	Transcription factor for the thyroid-specific expression of the genes
26	annexin A8	MALDI	1	22	P13928	an anticoagulant protein
27	glyceraldehyde-3-phosphate dehydrogenase (GAPDH)	MALDI	0.4	16	P04406	CATALYTIC ACTIVITY: D-glyceraldehyde 3-phosphate+phosphate+NAD^-=3-phospho-D-glyceroyl phosphate+NADH.
28	phosphoglycerate kinase 1 (PGK1)	WB			P00558	glycolytic enzyme, polymerase alpha cofactor protein
29	heterogeneous nuclear, ribonucleoprotein A1 (herix-destabilizing protein)	MALDI	0.4	30	P09651	Involved in the packaging of pre-mRNA into hnRNP particles, transport of poly(A) mRNA
30	elongation factor 1-α 1	MALDI	0.4	18	P68104	promotes the GTP-dependent binding of aminoacyl-tRNA to the A-site of ribosomes
31	transketolase	MALDI	0.4	8	P29401	CATALYTIC ACTIVITY: Sedoheptulose 7-phosphate+D-glyceraldehyde 3-phosphate=D-ribose 5-phosphate+D-xylulose 5-phosphate.
32	glyceraldehyde-3-phosphate dehydrogenase (GAPDH)	WB			P04406	CATALYTIC ACTIVITY: D-glyceraldehyde 3-phosphate+phosphate+NAD^-=3-phospho-D-glyceroyl phosphate+NADH.
33	α-enolase	WB			P06733	Multifunctional enzyme that, as well as its role in glycolysis
34	serine/threonine-protein kinase 13 (Aurora-C)	MALDI, WB	1	24	Q9UQB9	May play a part in organizing microtubules during mitosis
35	serine/threonine-protein kinase 13 (Aurora-C)	WB			Q9UQB9	May play a part in organizing microtubules during mitosis
36	voltage-dependent anion-selective channel protein 1 (VDAC-1)	WB			P21796	Forms a channel through the mitochondrial outer membrane and also the plasma membrane.
37	voltage-dependent anion-selective channel protein 1 (VDAC-1)	WB			P21796	Forms a channel through the mitochondrial outer membrane and also the plasma membrane.
38	voltage-dependent anion-selective channel protein 1 (VDAC-1)	WB			P21796	Forms a channel through the mitochondrial outer membrane and also the plasma membrane.
39	pyruvate kinase isozyme M2 (PKM2)	WB			P14618	CATALYTIC ACTIVITY: ATP+pyruvate=ADP+phosphoenolpyruvate.
40	pyruvate kinase isozyme M2 (PKM2)	WB			P14618	CATALYTIC ACTIVITY: ATP+pyruvate=ADP+phosphoenolpyruvate.
41	pyruvate kinase isozyme M2 (PKM2)	WB			P14618	CATALYTIC ACTIVITY: ATP+pyruvate=ADP+phosphoenolpyruvate.
42	pyruvate kinase isozyme M2 (PKM2)	WB			P14618	CATALYTIC ACTIVITY: ATP+pyruvate=ADP+phosphoenolpyruvate.
43	pyruvate kinase isozyme M2 (PKM2)	WB			P14618	CATALYTIC ACTIVITY: ATP+pyruvate=ADP+phosphoenolpyruvate.
44	pyruvate kinase isozyme M2 (PKM2)	WB			P14618	CATALYTIC ACTIVITY: ATP+pyruvate=ADP+phosphoenolpyruvate.
45	pyruvate kinase isozyme M2 (PKM2)	WB			P14618	CATALYTIC ACTIVITY: ATP+pyruvate=ADP+phosphoenolpyruvate.
46	pyruvate kinase isozyme M2 (PKM2)	WB			P14618	CATALYTIC ACTIVITY: ATP+pyruvate=ADP+phosphoenolpyruvate.
47	pyruvate kinase isozyme M2 (PKM2)	WB			P14618	CATALYTIC ACTIVITY: ATP+pyruvate=ADP+phosphoenolpyruvate.
48	phosphoglycerate kinase 1 (PGK1)	WB			P00558	glycolytic enzyme, polymerase alpha cofactor protein

The protein name listed in UniProt (SwissProt), identification method (ID method), mass tolerance used as activated parameter during MASCOT sever query, percent of the coverage (% coverage), accession number of the protein (Acc No), and function of the protein listed in UniProt (SwissProt) were shown.

tively. Protein spots clearly visualized by SYPRO Ruby staining were picked from the gels and subjected to the mass spectrometric analysis using a MALDI-TOF apparatus. Table 1 and Table 2 show the summary of the results. We could identify totally 45 and 48 protein spots in 2-DEs using pH 3–10 and pH 6–11 strips, respectively. These proteins were either components of cytoskeleton (tropomyosin-4, β-tubulin, vimentin, β-actin), enzymes involved in energy regulation (ATP synthase, L-lactate dehydrogenase, α-enolase, transketolase, phosphoglycerate mutase, TIM, GAPDH, PKM2, PGK1), proteins involved in redox regulation (peroxiredoxin, glutathione S-transferase, thioredoxin reductase), chaperones (T-complex protein, heat shock proteins, calreticulin precursor), components of the translation machinery (elongation factors 1 and 2), regulators of dynamisms in nuclear events (prohibitin, nucleolin, GTP-binding nuclear protein Ran, Aurora-C), apoptosis-related proteins (VDAC-1, annexin A5) or adaptor proteins (14-3-3 ε and 14-3-3 ζ). These proteins are major actors required for cell survival in general. An exception is pigment epithelium-derived factor, a neurotrophic factor that induces extensive neuronal differentiation in retinoblastoma cells. Its expression in undifferentiated ES cells might explain, at least in part, the well-known characteristics of mammalian ES cells that they prone to undergo neuronal differentiation when signals required for the maintenance of undifferentiated states are eliminated.

We next performed the two-dimensional western blotting to confirm the results of mass spectrometry using commercially available polyclonal antibodies having wide cross-reactivity concerning HSP60, Annexin A5, HSC70, TIM, 14-3-3 ε and 14-3-3 ζ, α-enolase, GAPDH, annexin A2, VDAC-1, PKM2, PGK1 and Aurora-C. As shown in Fig. 2 and Fig. 3, each protein spot was eventually recognized by the corresponding antibody, proving the validity of the MALDI-TOF-based protein identification process using human databases. On the other hand, usage of non-human primate databases, in which cynomolgus monkey's data are included, provided no better information. They seldom gave us candidate proteins or only gave the same candidate as

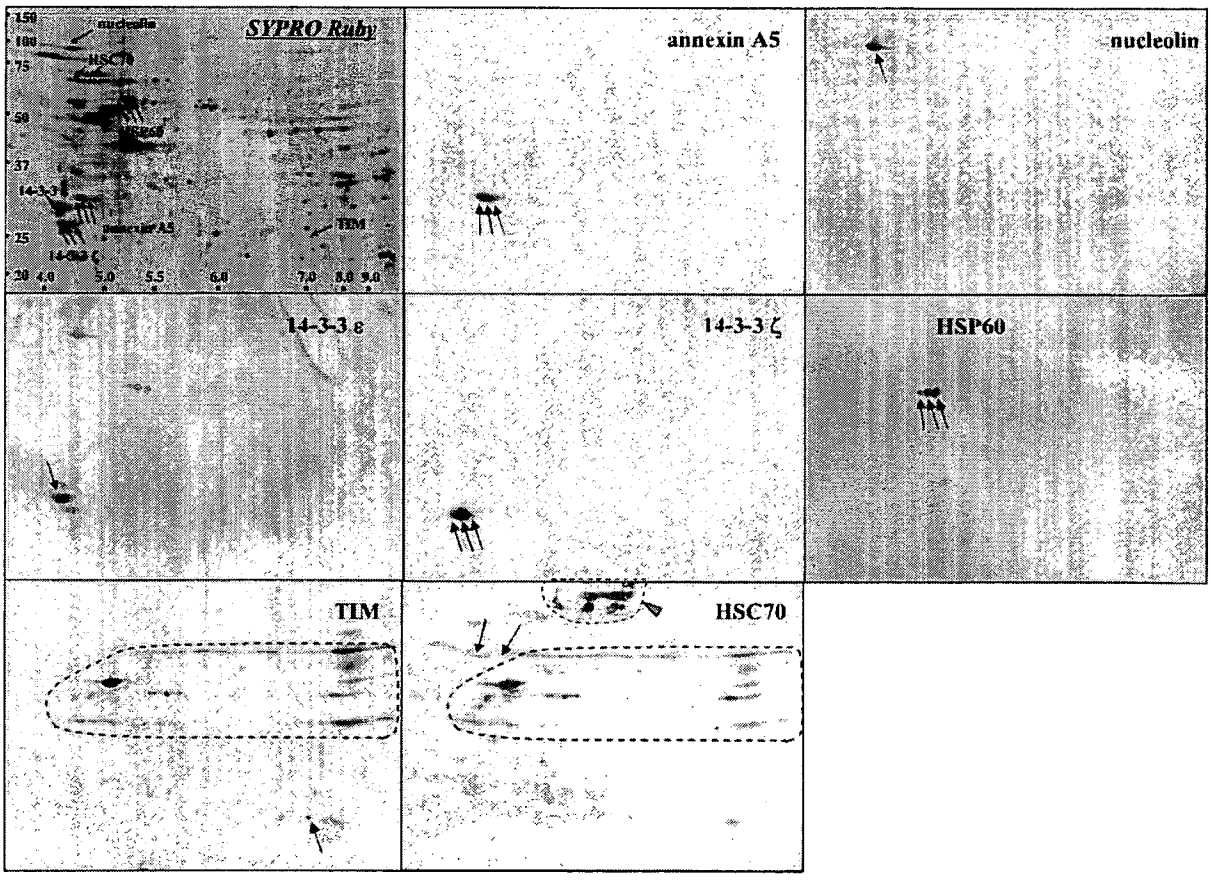

Fig. 2. Two dimensional western blotting after a pH 3–10 strip-using 2-DE gel.

The 2-DE gel was trimmed (an upper left panel) and transferred to the PVDF membrane. Western blotting was performed using indicated polyclonal antibodies, which are shown to have broad cross-reactivity among human, mouse and rat by the manufacturer. The PVDF membrane was re-used after stripping the previously used antibody. The multiple spots and slurs in an area surrounded by a dotted line in TIM and HSC70 antibody reactions are the background spots created during the anti-TIM antibody reaction. The irregular marks in the area shown by a dotted line with a gray arrowhead in anti-HSC70 antibody reaction are non-specific stains created during this antibody reaction.